Journal of Hazardous Materials 267 (2014) 183–193

Contents lists available at ScienceDirect

Journal of Hazardous Materials

journal homepage: www.elsevier.com/locate/jhazmat

Particle concentration dynamics in the ventilation duct after an artificial release: For countering potential bioterrorist attack

Siming You, Man Pun Wan*

School of Mechanical and Aerospace Engineering, Nanyang Technological University, 50 Nanyang Avenue, 639798, Singapore, Singapore

HIGHLIGHTS

- Potential ways of harmful agents releasing in the ventilation duct are identified.
- Models of particle concentration dynamics for these releasing events are proposed.
- A series of wind tunnel experiments are conducted to validate the proposed models.
- The models provide the basis for assessing risk of harmful agents releasing events.
- Indoor airborne particle concentration models were derived.

ARTICLE INFO

Article history:
Received 30 July 2013
Received in revised form
27 December 2013
Accepted 30 December 2013
Available online 6 January 2014

Keywords:
Bioterrorist attack
Ventilation duct
Concentration dynamics model
Resuspension
Injection

ABSTRACT

Ventilation duct serves as a potential target for bioterrorist attack. Understanding the dynamics of aerosolized harmful agents in the ventilation ducts provides the fundamentals for effective control and management, e.g., risk assessment. In this work, new models for predicting the concentration dynamics in the ventilation duct after a particle resuspension (representing the case that harmful agents are dosed when the ventilation is off and subsequently being turned on) or puff injection (representing the case that harmful agents are dosed when the ventilation is running) event were derived based on the mass balance model. The models were validated by a series of wind tunnel experiments. Indoor airborne particle concentration models were derived by incorporating the proposed ventilation duct models for resuspension and injection cases. The effects of resuspension and injection in the duct on indoor airborne particle concentration were examined by two hypothetical cases of *Bacillus anthracis* dosage using the derived models. For the same amount of BW agent dosage in the ventilation duct, the resuspension type release prolongs the exposure of harmful agents whereas the injection type release produces a higher peak concentration.

1. Introduction

The bioterrorist attack by the intentional release of biological weapons (BW) (e.g., viruses and bacteria) has drawn increasing attention worldwide since the anthrax letter attack of 2001 in the United States. The bioterrorist attack, once occurs, could produce great panic in the public due to its potential for causing massive civilian casualties. The economic impact of a bioterrorist attack could be as high as about $26.2 billion per 100,000 persons exposed to BW agents, suggesting the great economic burden to the society [1]. Hence, it is necessary to have effective measures to mitigate the attack once it happens. As one of important measures, the risk assessment of bioterrorist attack could provide useful information for defending against and mitigating the attack [2]. However, a robust risk assessment requires the knowledge about how BW agents are transmitted in the environment [3,4].

Recently, the United States government has warned that the ventilation systems of buildings are an ideal target for bioterrorism [5]. Actually, there was evidence showing that some terrorists were trained to inject harmful agents toward the air intake of a building [6]. Previous study [7] identified the role of ventilation duct in the dispersion of anthrax spores and indicated that even a small amount release of spores could be distributed throughout a high-rise building. However, there are still limited studies assessing the risk of bioterrorist attack through ventilation systems. The accurate risk assessment of ventilation-duct-based attack is further limited by the poor knowledge about the agent concentration variation in the duct. Hence, a model that can predict the dynamics of BW agent concentration in the ventilation duct after a deliberate release is of fundamental importance. Such model allows the prediction of indoor BW agent concentration and thus the exposure of residents to the agents.

* Corresponding author. Tel.: +65 67905498; fax: +65 6792 4062.
E-mail addresses: mpwan@ntu.edu.sg, manpunwan@gmail.com (M.P. Wan).

0304-3894/$ – see front matter © 2014 Elsevier B.V. All rights reserved.
http://dx.doi.org/10.1016/j.jhazmat.2013.12.058

The bioterrorist attack through ventilation systems can be accomplished by two ways. Firstly, terrorists could deliberately place the BW agents onto the duct surface when the ventilation system is off (usually at night, therefore more covert). Some of these agents could be resuspended and transported into indoor environment once the ventilation is running, leading to mass contamination, as suggested by the existing studies [8–10]. Secondly, it is possible that the BW agents are directly injected into the duct when the ventilation is running. Some of these injected agents would be instantly transported into indoor environment along with the airflow, causing mass contamination.

Few studies have been conducted to investigate the particle concentration dynamics in the ventilation duct following a BW agent resuspension or injection event. Until recently, Zhou et al. [11] proposed a model for the particle concentration dynamics in the ventilation duct considering resuspension. However, their model was constructed based on the assumption that both the particle deposition and resuspension occur uniformly along the whole length of ventilation duct. This naturally makes their model inappropriate for cases where high concentration of particles are dosed in a small area in the duct and the initial resuspension occurs from that small area, usually in the case of bioterrorist attack. The governing equation in [11] was specifically organized to have a term accounting for the particle resuspension along the whole length. In the case of resuspension from a small area, this governing equation in [11] no longer holds and a simple substitution of the resuspension term in the governing equation is not physically reasonable. A different method is needed to solve the new governing equation corresponding to the case that initial resuspension occurs from a small area. Based on the mass balance approach, this work proposed new models for particle concentration dynamics in the ventilation duct following a resuspension or injection event. The proposed models were validated by a series of wind tunnel experiments. Indoor airborne particle concentration models were then derived by incorporating the proposed ventilation duct models for resuspension and injection cases. The effects of resuspension and injection in the duct on indoor airborne particle concentration are examined, respectively, by two hypothetical cases using the derived models.

2. Model derivation

2.1. Model for particle resuspension case

This part of model derivation concerns the case that particles (BW agents) are dosed into the ventilation duct when the ventilation system is off. The particles deposit (primary deposition) on a small area in the duct and are subsequently resuspended (primary resuspension) into the airflow stream when the ventilation is turned on. Only the initial (primary) resuspension is considered here, because (1) it plays the dominant role in affecting the airborne particle concentration over the secondary resuspension (subsequent resuspension of particles deposited on the duct surface downstream); (2) the amount of particles for secondary deposition is small and the amount for secondary resuspension would be even far smaller than that for secondary deposition, meaning that the net deposition could be well approximated by the secondary deposition; (3) the further consideration of the secondary resuspension will be a traversal problem that is prohibitive to solve. It is assumed

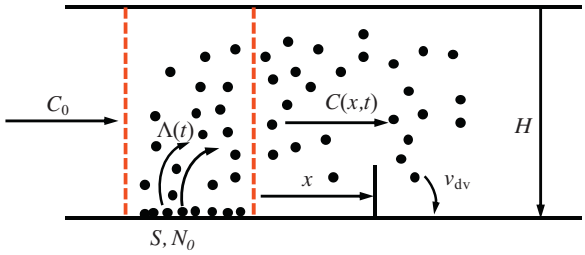

Fig. 1. A schematic of the particle resuspension in a duct.

that the length of the ventilation duct is much larger than the height and width of the duct. The transient particle concentration variation along the stream-wise direction$C(x,t)$ is concerned in the proposed model. The dimensions of the cross section of the wind tunnel's test section is 20 cm (W) × 20 cm (H) For such cross sectional dimension, the particle concentration variation in the bulk flow in the transverse direction of the cross-sectional plane is generally within a factor of 5 as shown previously [12,13]. Hence, particle concentration is assumed homogenous in the cross-section at any given point in x and t for simplifying the model development. Similar assumption was also adopted in the model of Zhou et al. [11]. As shown in Fig. 1, the particle resuspension occurs within the area of S (dose area of BW agents) where the particle surface number concentration is N_0. The particle concentration upstream the resuspension area is C_0, while the particle concentration downstream the resuspension area is $C(x,t)$. According to the conservation of mass, the mass balance model about $C(x,t)$ can be written as:

$$A\frac{\partial C(x,t)}{\partial t} + Q_s\frac{\partial C(x,t)}{\partial x} = -v_{dv}C(x,t)P \tag{1}$$

with the boundary condition of

$$C(x,t)|_{x=0} = C_0 + \frac{N_0 S\Lambda(t)}{Q_s} \tag{2}$$

and the initial condition of

$$C(x,t)|_{t=0} = C_{t0}, \tag{3}$$

where A is the cross sectional area of duct, Q_s is the volumetric flow rate, v_{dv} is the particle deposition velocity, P is the cross sectional perimeter of duct and Λ is the particle resuspension rate defined as the fraction of particles resuspended per unit time. The resuspension rate generally has a power law relationship versus time: $\Lambda(t) = r_1 t^{-r_2}$ [14–16]. After plugging the resuspension rate expression into Eq. (1), the solution of Eq. (1) is derived as (see Appendix A):

$$C(x,t) = \begin{cases} C_{t0}e^{-\frac{v_{dv}Pt}{A}} & \left(0 < t \le \frac{Ax}{Q_s}\right) \\ \frac{N_0 S r_1}{Q_s\left(t - Ax/Q_s\right)^{r_2}}e^{-\frac{v_{dv}Px}{Q_s}} + C_0 e^{-\frac{v_{dv}Px}{Q_s}} & \left(\frac{Ax}{Q_s} < t\right) \end{cases}. \tag{4}$$

In Eq. (4), Ax/Q_s defines the time when the location x will be affected by the resuspended particles. That is, when $0 < t \le Ax/Q_s$, the location x will have a concentration variation affected by the deposition only. Otherwise, the location x will have a concentration variation influenced by both particle resuspension and deposition.

Considering that the particle deposition velocities onto floor, wall and ceiling are different due to the effect of gravity, Eq. (4) is modified to

$$C(x,t) = \begin{cases} C_{t0}\ \exp(-(v_{dfv}P_f + v_{dwv}P_w + v_{dcv}P_c)t/A) & \left(0 < t \le \frac{Ax}{Q_s}\right) \\ \frac{N_0 S r_1}{Q_s\left(t - Ax/Q_s\right)^{r_2}}\exp(-(v_{dfv}P_f + v_{dwv}P_w + v_{dcv}P_c)x/Q_s) + C_0\exp(-(v_{dfv}P_f + v_{dwv}P_w + v_{dcv}P_c)x/Q_s) & \left(\frac{Ax}{Q_s} < t\right) \end{cases}, \tag{5}$$

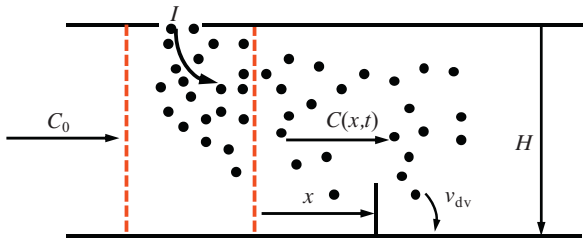

Fig. 2. A schematic of the particle injection in a duct.

where v_{dfv}, v_{dwv} and v_{dcv} are the deposition velocities of particles onto the floor, wall and ceiling of duct, respectively, and P_f, P_w and P_c are the width of floor, wall and ceiling, respectively. The estimation of deposition velocities onto different surfaces of duct will follow the reported method [17]. The particle surface number concentration N_0 is calculated as

$$N_0 = \frac{M_{0r} f}{Sm}, \tag{6}$$

where M_{0r} is the mass of particles released to the surface for resuspension. $m = \pi/6 d_p^3 \rho_p$ is the mass of a particle with diameter d_p and density ρ_p. f denotes the fraction of deposited particles belonging to the size bin of d_p, which can be obtained from the particle size distribution. The resuspension rate is estimated based on the previous empirical models of Loosmore [15] or Kim et al. [14]. Two models and three models have been developed in [15] and [14], respectively. Because the different models from the same study generally produced similar results, one model from each of these studies was selected for the comparison purpose: emp1 (denoted as Model 1) from [15] and Model II-A (denoted as Model 2) from [14].

$$\text{Model 1:} \qquad \Lambda = 0.42 \frac{u^{*2.13} d_p^{0.17}}{t^{0.92} R_q^{0.32} \rho_p^{0.76}} \tag{7}$$

and

$$\text{Model 2:} \qquad \frac{\Lambda d_p}{u^*} = 8.521 \times 10^{-3} \left(\frac{\rho_p}{\rho_a}\right)^{-0.3028} \left(\frac{u^* t}{d_p}\right)^{-1.0135} \left(\frac{R_q}{d_p}\right)^{-0.3269} \left(\frac{A_{132}}{d_p^3 u^{*2} \rho_a}\right)^{-0.2961}, \tag{8}$$

where t is the time, ρ_a is the density of air, R_q is the roughness of surface, u^* is the friction velocity and A_{132} is the Hamaker constant.

2.2. Model for particle injection case

For the injection case (Fig. 2), the same mass balance model (Eq. (1)) holds but the boundary condition is modified to

$$C(x,t)|_{x=0} = \begin{cases} C_0 + \dfrac{I}{Q_s} & (0 < t < T) \\ C_0 & (t \geq T) \end{cases}, \tag{9}$$

where I is the number of particles injected into the duct per unit time and could be estimated by n/T with T the injection duration and $n = fM_{0i}/m$ the number of injected particles within a certain size bin during the period of T. M_{0i} is the total mass of particles injected into the duct. Corresponding to Eq. (9), the solution of Eq. (1) could be derived following a similar procedure as

$$C(x,t) = \begin{cases} C_{t0} e^{-\frac{v_{dv} P t}{A}} & \left(0 < t \leq \dfrac{Ax}{Q_s}\right) \\ \left(C_0 + \dfrac{I}{Q_s}\right) e^{-\frac{v_{dv} P x}{Q_s}} & \left(\dfrac{Ax}{Q_s} < t < \dfrac{Ax}{Q_s} + T\right) \\ C_0 e^{-\frac{v_{dv} P x}{Q_s}} & \left(\dfrac{Ax}{Q_s} + T \leq t\right) \end{cases}. \tag{10}$$

The solution suggests that the concentration variation at the location x responds like a pulse function versus time. As $Ax/Q_s < t < Ax/Q_s + T$, the location x will be affected by both particle injection and injection. Considering the different deposition velocities of particles onto the different surfaces of duct, Eq. (10) is modified to:

$$C(x,t) = \begin{cases} C_{t0} \exp(-(v_{dfv}P_f + v_{dwv}P_w + v_{dcv}P_c)t/A) & \left(0 < t \leq \dfrac{Ax}{Q_s}\right) \\ \left(C_0 + \dfrac{I}{Q_s}\right) \exp(-(v_{dfv}P_f + v_{dwv}P_w + v_{dcv}P_c)x/Q_s) & \left(\dfrac{Ax}{Q} < t < \dfrac{Ax}{Q_s} + T\right) \\ C_0 \exp(-(v_{dfv}P_f + v_{dwv}P_w + v_{dcv}P_c)x/Q_s) & \left(\dfrac{Ax}{Q_s} + T \leq t\right) \end{cases}. \tag{11}$$

The estimation of deposition velocities onto different surfaces will also follow the method of [17].

3. Validation experiments

3.1. Particle resuspension experiments

3.1.1. Roughness measurement

The roughness of substrate is required to estimate the resuspension rate with Eqs. (7) and (8). In the resuspension experiments, three types of materials (stainless steel, aluminum and plastic) were tested, as they are commonly used materials for ventilation duct [18–21]. 5 pieces of 4 cm × 4 cm square-shaped substrate were prepared from each material and the roughness of each substrate was measured using a surface roughness tester (Mitutoyo, SJ301) at three random locations. The averaged root mean square (RMS) roughness for each material was listed in Table 1. The other material properties required for the resuspension rate calculation are also given in Table 1.

3.1.2. Sample preparation

A deposition chamber was used to load the test particles (ISO 12103-1 A1 Arizona test dust) onto the substrates to mimic BW agent dose during ventilation off period. The deposition procedure is similar to the one described in [25]. The loaded substrates would be used for the subsequent resuspension experiments in the wind tunnel. The size of test particles ranges from 1 to 10 μm which covers the size ranges of some common BW agents such as *Bacillus*

Table 1
The parameters required for the resuspension rate estimation.

	u^*(m/s)	ρ_p (kg/m^3)	ρ_a (kg/m^3)	d_p(μm)	R_q(μm)	A_{132}[a](×10^{-20}J)
Aluminum	0.278	2650	1.2	2/4.75	0.44	15.7
Stainless steel	0.278	2650	1.2	2/4.75	0.09	2.7
Plastic	0.278	2650	1.2	2/4.75	0.02	7.3

[a] $A_{132} = \sqrt{A_{11}A_{22}}$, with A_{11} the Hamaker constant of substrate and $A_{22} = 6.8 \times 10^{-20}$ J the Hamaker constant of particles [14]. The Hamaker constants for aluminum, stainless steel and plastic are 36.0×10^{-20}[22], 1.0×10^{-20}[23] and 7.8×10^{-20} J [24], respectively.

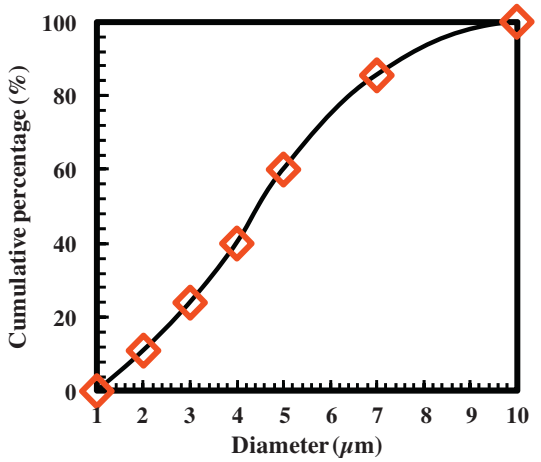

Fig. 3. The cumulative size distribution of particles.

anthracis and *Botulinum toxin* [26]. The cumulative size distribution of particles in terms of volume is shown by Fig. 3. The weights of each piece of substrate before and after the deposition procedure were measured by an analytical balance (Radwag XA 110/X) and denoted as M_{1r} and M_{2r}, respectively. The deposited mass of particles is calculated as $M_{0r} = M_{2r} - M_{1r}$ and listed in Table 2. More details about the deposition chamber and procedure could be found in [25].

3.1.3. Resuspension experiments

Resuspension experiments were conducted in a suckdown wind tunnel setup (Fig. 4) with a test section of 20 cm (W) × 20 cm (H) × 100 cm (L). A flow straightener was installed in front of the contraction part to smooth flow and the turbulators were paved behind the contraction part to induce a turbulent boundary layer. A 23.5 cm (L) × 20.0 cm (W) supportive plastic substrate base with a 4.0 cm (L) × 4.0 cm (W) trough for fitting the test substrate was fixed in the test section. The distance between the center of the trough and the inlet of the test section was 48.5 cm. The substrate base has a 10° wedge to allow smooth change of flow direction. The speed of fan (Kruger Engineering Pte Ltd, FSA200/CM), i.e., the free stream velocity, was controlled by a frequency inverter. An aerosol spectrometer (Grimm, model 1.109) was employed with the probe 15 cm downstream the substrate to measure the particle concentration at the sampling interval of 6 s. The height of the probe from the floor of test section was 9 cm. This one-point measurement approach was adopted based on the assumption that particle concentration is homogeneous in the cross-sectional plane, as adopted in the model derivation. The experimental uncertainties that could potentially be introduced by the cross-sectional homogeneous assumption and one-point measurement approach will be discussed in Section 4.1.3.

Before the resuspension experiment, the relationship between the friction velocity (required for resuspension rate calculation) and free stream velocity was determined based on the boundary layer velocity profile measured with a set of hot wire anemometer (developed by The University of Newcastle). A height gauge (Mitutoyo, series 192) was used to control the vertical movement of the anemometer probe. A pitot-tube with an inclined manometer (Airflow Developments Ltd) was used to measure the free stream velocity and calibrate the hot wire anemometer. The detailed procedure of determining the friction velocity is given in Appendix B. A linear relationship between the friction velocity and free stream velocity was found as $u^* = 0.0710u - 0.0056$ with the residual sum of square $R^2 = 0.988$.

The free stream velocity of 4.0 m/s (Re = 53,000) was used during the resuspension experiments, which fell into the range of common free stream velocities in the ventilation ducts (2–9 m/s and $Re \approx 20,000 - 60,000$) [27]. An annular aspiration inlet was employed for particle sampling. Under the free stream velocity of 4.0 m/s, the overall sampling efficiency of the inlet was estimated to be larger than 95% for particles smaller than 10 μm in size, according to the existing theory [28]. This suggested that an approximately isokinetic sampling condition was achieved. At the beginning of each resuspension experiment, the background concentration, the average of which served as the upstream concentration C_0 (Table 2) for the model prediction, was measured for 2 min. The substrate was then mounted on the substrate base in the wind tunnel for the resuspension experiment and the particle concentration in the tunnel was measured for another 2 min. For each material, all 5 pieces of substrate were tested in the resuspension experiments and the measured concentrations for them were averaged for the model validation. The relative humidity and temperature in the wind tunnel were measured to be 85% ± 2% and 27 °C ± 2 °C, respectively, using a RH-temperature sensor (OMEGA, RH-USB).

3.2. Injection experiments

For the injection experiments, the substrate base used for the resuspension experiments was taken out from the test section of wind tunnel. A circular inlet port being 0.5 m upstream the

Table 2
The deposited and injected mass of particles and the upstream particle concentration.

		M_{0r}/M_{0i} (g)	C_0 (#/m^3)		
			2 μm	4.75 μm	8.25 μm
Resuspension	Aluminum	0.01161 (0.00357)[a]	201,650 (50,010)	5817 (2007)	–
	Stainless steel	0.01290 (0.00475)	225,252 (72,351)	3306 (1691)	–
	Plastic	0.01347 (0.00480)	200,367 (20,991)	4282 (1670)	–
Injection	–	0.02611 (0.00895)	261,780 (59,166)	6600 (2427)	540 (214)

[a] The standard deviations are shown within brackets.

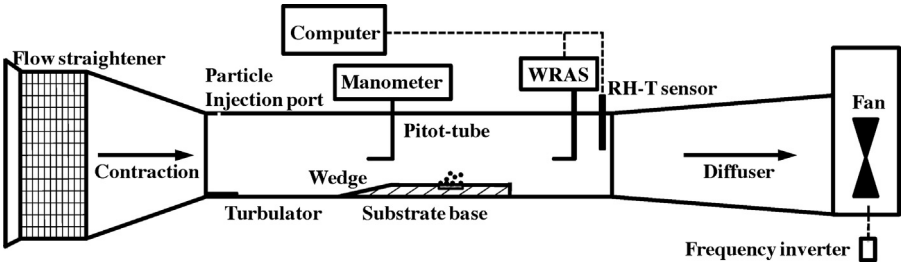

Fig. 4. A schematic of the wind tunnel setup.

spectrometer probe was drilled at the ceiling of the test section. The test particles were injected into the test section through the inlet port with a syringe. The free stream velocity of 2.5 m/s was used for the injection experiments. Just before the injection experiment, the weight (M_{1i}) of syringe loaded with particles was measured with the analytical balance. The background concentration was measured for 2 min firstly, the average of which served as the upstream concentration C_0 (Table 2) for the model predictions. Then, the particles were slowly injected into the tunnel by pushing the rod of syringe at an even rate of 15 times/min for 1 min. After the injection, the particle concentration was measured for two more minutes and the syringe was again sent to the balance for the weight measurement (M_{2i}). The mass of injected particles was calculated as $M_{0i} = M_{1i} - M_{2i}$, which was used to estimate the number of injected particles, n, in Eq. (9). The test section was then cleaned before a new run of experiment. A total of five runs of experiments were conducted and the data of all five runs were averaged for the model validation.

4. Results and Discussion

4.1. Model validation

4.1.1. Resuspension case

In the resuspension case, the time limit, Ax/Q_s, (Eq. (5)), is equal to 0.0375 s, suggesting that the resuspended particles would pass the measurement point within a negligibly short period of time compared with the sampling interval of 6 s. Therefore, the concentration variation as $0 < t \leq Ax/Q_s$ in Eq. (5) is not considered in the following validation. The concentration variations due to the resuspension for the particles larger than 6.5 μm are very small, therefore they are not considered in the validation for the statistical significance of analysis. The considered particles were divided into 2 size bins: 1–3, 3–6.5 μm, with the denoted mean diameters of 2 and 4.75 μm, respectively. The estimated resuspension rates and deposition velocities of various cases are shown in Table 3. The model validation is shown by Fig. 5. Since the measurement interval of spectrometer is 6 s, the time axis starts from 6 s in Fig. 5.

It is shown that the concentration dynamics after the particle resuspension is reasonably captured by the proposed model. Both the experimental and modeling results show that the particle concentration becomes 1.5–3 times and 4–8 times higher than the upstream one immediately after the initiation of airflow for 2 μm and 4.75 μm particles, respectively, and gradually decreases afterwards. Once the airflow was initiated, the airflow resuspended the particles on the substrate and quickly pushed them forwards the measurement point, leading to the significant concentration increase. The subsequent concentration decline was mainly caused by three aspects based on the proposed model: (1) the resuspension rate decreases as the time goes on; (2) the ventilation continuously refreshes the air in the tunnel (dilution effect); (3) some of the resuspended particles deposit onto the duct surfaces. Actually, it could be expected that the particle concentration should be asymptotic to the upstream one, C_0.

The comparison between the model predictions based on the empirical resuspension model of [15] (Model 1) and that based on the one of [14] (Model 2) shows that the latter-based model provides larger but generally better predictions than former-based model. The larger predictions for the Model 2-based model correspond to the calculated larger resuspension rate coefficient, r_1 (Table 3).

4.1.2. Injection case

Similar to the resuspension case, the concentration variation as $0 < t \leq Ax/Q_s$ is also disregarded in the injection case. The particles were divided into 3 size bins: 1–3, 3–6.5 and 6.5–10 μm with the denoted mean diameters of 2, 4.75 and 8.25 μm, respectively. The estimated deposition velocities for various cases are listed in Table 3. The model validation is shown by Fig. 6.

It is shown that the trend of particle concentration variation during and after particle injection is reasonably predicted by the model. The difference between model predictions and experimental data generally fall within a range of 30%. The model overestimates the concentration for the larger particles (4.75 and 8.25 μm) during the injection period by a factor of 1.3 which is larger than that (a factor of 1.1) for the smallest particles (2 μm). This should be related to the larger inertia of the larger particles, leading to worse mixing of particles in the air stream before reaching the measurement point. The measured concentration shows a slight growth within the initial 6–12 s which is not predicted by the model. This initial growth period might correspond to (1) the time taken to reach steady measurement for the spectrometer for a sudden concentration increase, as observed previously [29,30], and (2) the time taken to make the injection steady. Once the particle injection ceases, the concentration quickly decreases to the upstream level due to the dilution effect of ventilation in the duct.

The comparison between Figs. 5 and 6 shows that the patterns of concentration variation between the resuspension and injection cases are entirely different. Although the amount of particles injected into the tunnel is about double of that deposited onto the substrate, the fraction of particles transported downstream in the injection case is about 2–3 orders of magnitude larger than that in the resuspension case. Hence, it is necessary to correctly identify the actual way of particle release for a bioterrorist attack and take the control and prevention measures (e.g., risk assessment) correspondingly, and the proposed models could potentially serve as such a tool of indentifying the way of release.

A uniform particle injection was used in the current work for the ease of data analysis and the repeatability of experiments. In real situations, the particle may not necessarily be injected uniformly but intermittently into the ventilation duct. However, the manner of concentration variation could still be speculated based on the proposed model. Although the particle injection may not be uniform over the whole injection period, it could be approximately uniform over small enough time lengths. The concentration

Table 3
The resuspension rates and deposition velocities of various cases.

I Experimental cases			Resuspension						Injection		
			Aluminum		Stainless steel		Plastic				
d_p (μm)			2	4.75	2	4.75	2	4.75	2	4.75	8.25
$\Lambda = r_1 t^{-r_2}$	Model 1	r_1	0.0008	0.0009	0.0013	0.0015	0.0022	0.0025			–
		r_2	0.92	0.92	0.92	0.92	0.92	0.92			
	Model 2	r_1	0.0018	0.0053	0.0052	0.0151	0.0063	0.0183			
		r_2	1.0135	1.0135	1.0135	1.0135	1.0135	1.0135			
v_{dfv} (m/s)			0.0014	0.0058	0.0014	0.0058	0.0014	0.0058	0.0004	0.0022	0.0063
v_{dwv} (m/s)			0.0005	0.0018	0.0005	0.0018	0.0005	0.0018	0.0001	0.0002	0.0005
v_{dcv} (m/s)			0.0010	0.0031	0.0010	0.0031	0.0010	0.0031	0.0003	0.0007	0.0012

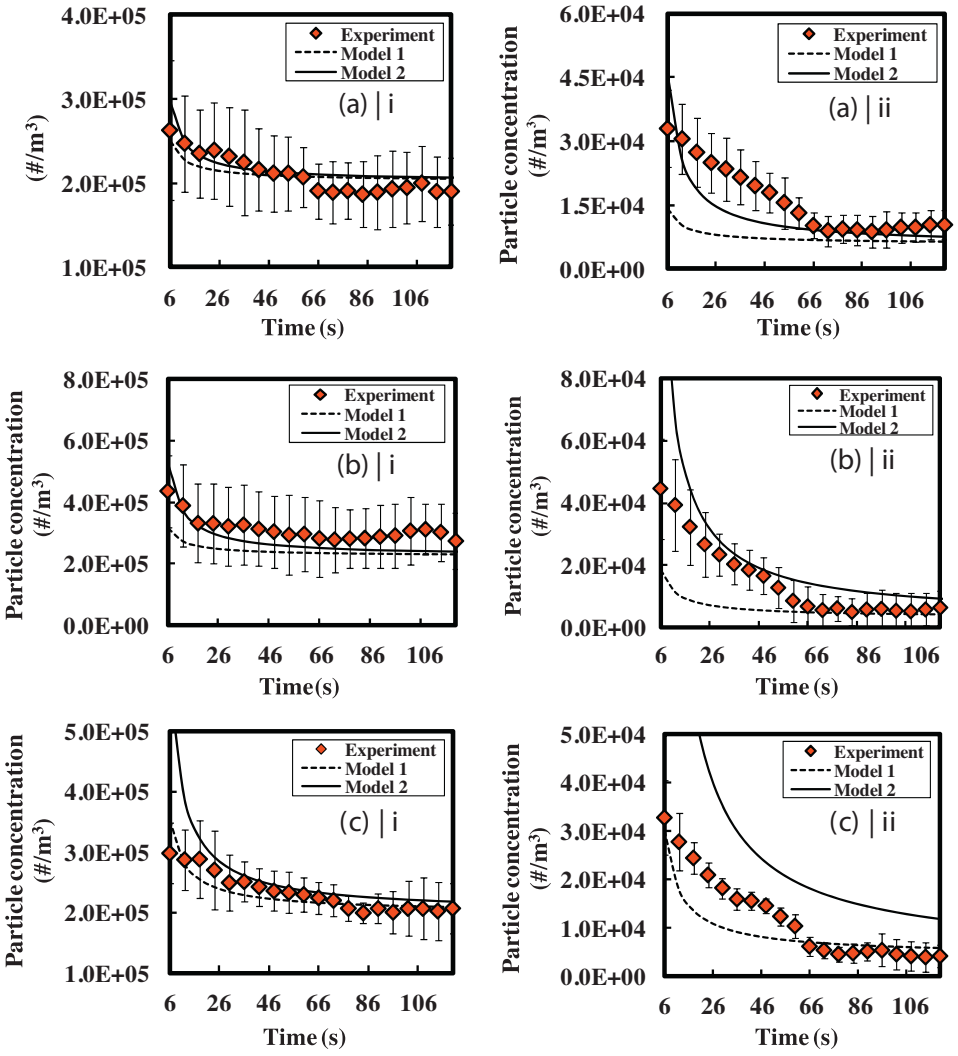

Fig. 5. The comparison between the measured and modeled concentration variations after particle resuspension for the substrates of (a) aluminum (i: 2 μm; ii: 4.75 μm), (b) stainless steel (i: 2 μm; ii: 4.75 μm) and (c) plastic (i: 2 μm; ii: 4.75 μm). The error bars denote one standard deviation.

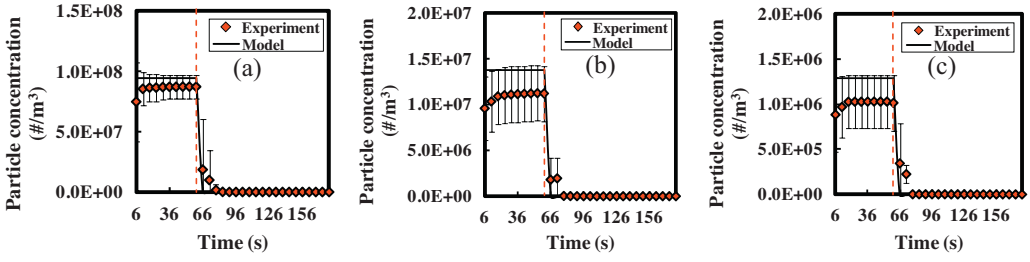

Fig. 6. The comparison between the measured and modeled concentration variations: (a) 2 μm; (b) 4.75 μm; (c) 8.25 μm. The error bars denote one standard deviation. The vertical dash line at 60 s indicates the time of stopping the particle injection.

variation over the whole injection period would be the combination of the variations over these smaller time lengths following the proposed model. Therefore, the concentration would behave like a fluctuated rectangular pulse function during the injection period and restore to the background concentration after injection. Furthermore, for the risk assessment, it is important to know the amount of particles entering indoor environment from the ventilation system. The assumption of uniform injection actually will not affect the estimation of the amount of particles entering indoors once the amount of injected particles is set whatever the injection method is. Therefore, the proposed model for uniform injection is still suitable for the future risk analysis by regulating the amount of injected particles in the model.

4.1.3. Potential uncertainties associated with the cross-sectional homogeneous assumption

It is should be noted that particle concentration is assumed homogenous in the cross-section in the current models. In order to further model the potential spanwise and transverse concentration variations, it is necessary to understand the three-dimensional flow field in the duct. A model based on CFD simulation could serve as the potential solution for such purpose, which will be beyond the scope of the current study and left for the future study. CFD-based models have the potential to achieve a higher accuracy by modeling three-dimensional concentration distribution and allow tracking of pathogens. However, CFD-based models require significantly more computational effort and thus time than the models developed in this work, while time is critical for post-attack responses.

One potential uncertainty from the homogeneous concentration assumption could have been reflected in the standard deviations of experimental data used for model validation. As shown above, the experimental data bear the standard deviation up to 30% of the mean for both resuspension and injection cases. This uncertainty of experimental data may have been resultant from the one-point measurement under the homogeneous concentration assumption. Another potential uncertainty that could be induced by the homogeneous concentration assumption is the estimation of the effect of particle deposition onto duct surfaces, that is, the deposition effect. However, the effect of deposition on particle concentration variation is minor under the settings considered in this study (as inferred from the results discussed in Appendix C). It is believed that the homogeneous particle concentration assumption has limited effect on the estimation of the total amount of particles that enter indoors following a resuspension or injection event. As a result, the practical application of the developed models will not be affected by the assumption of uniform cross-sectional concentration.

4.2. Model application

4.2.1. Indoor airborne particle concentration modeling

The application of the ventilation duct models (resuspension and injection) developed in Section 2 for indoor particle concentration prediction is demonstrated by incorporating the ventilation duct models into the indoor airborne mass balance model based on well-mixed assumption. The well-mixed assumption was widely adopted for modeling indoor particle concentration dynamics [31–34]. The indoor airborne mass balance model is

$$\frac{dC_i}{dt} = aC_{ov} - bC_i \tag{12}$$

with the initial condition of $C_i(0)$. C_i is the indoor airborne particle concentration. C_{ov} is the particle concentration in the ventilation duct from a resuspension or injection event. a is the entrance rate of the resuspended or injected particles from the duct. $a = (1 - R_r)(1 - \eta_r)d_v p_b \alpha_a$. α_a is the air exchange rate. R_r is the recirculation fraction of indoor exiting air. η_r is the removal efficiency of filter in the duct and could be obtained from the study of Riley et al. [35] for some commonly used commercial filters (e.g., 40% and 85% ASHRAE filters). $d_v = \exp\left(-(\nu_{dfv}P_f + \nu_{dwv}P_w + \nu_{dcv}P_c)x/(1 - R_r)Q_s\right)$ is the parameter accounting for the effect of particle deposition in the ventilation duct as suggested by Eqs. (5) and (11). p_b is the aerosol penetration through bends for the resuspended or injected particles in the ventilation duct and could be estimated by the model proposed by McFarland et al. [36]. $b = \alpha_a - R_r d_{vi}(1 - \eta_r)p_{bi}\alpha_a + \left((\nu_{df}A_f + \nu_{dw}A_w + \nu_{dc}A_c)/V\right) + \left(\beta_b n_p/V\right)$ is the loss rate of indoor particles ν_{df}, ν_{dw} and ν_{dc} are the particle deposition velocities onto the indoor floor, wall and ceiling, respectively, and can be estimated by the model of Lai and Nazaroff [37] or by experimental data [38]. A_f, A_w and A_c are the areas of indoor floor, wall and ceiling, respectively. β_b is the breathing rate of occupant. n_p is the number of occupants. V is the volume of indoor space $d_{vi} = \exp\left(-\left((\nu_{dfv}P_f + \nu_{dwv}P_w + \nu_{dcv}P_c)x_{vi}/R_r Q_s\right)\right)$ accounts for the effect of particle deposition in the ventilation duct for the particles in the recirculated air x_{vi} is the duct length passed by the recirculated air p_{bi} is the aerosol penetration through bends in the ventilation duct for the particles in the recirculated air $Q_s = \alpha_a V$ is the ventilation rate.

In the resuspension case, C_{ov} is obtained from the developed model, Eq. (5) as

$$C_{ov} = \frac{N_0 S r_1}{Q_s t^{r_2}} + C_0 \tag{13}$$

The terms accounting for the deposition effect are not included, because they have been considered by a in the mass balance model. Substituting Eq. (13) into Eq. (12) and rearranging yield

$$\frac{dC_i}{dt} + bC_i = a\left(\frac{N_0 S r_1}{Q_s t^{r_2}} + C_0\right) \tag{14}$$

The solution to Eq. (14) is

$$C_i(t) = e^{-bt}C_i(0) + \frac{aC_0}{b}\left(1 - e^{-bt}\right) + \frac{aN_0 S r_1}{Q_s}e^{-bt}\int_0^t \frac{e^{bt}}{t^{r_2}}dt \tag{15}$$

In the injection case, C_{ov} is obtained from the developed model, Eq. (11) as

$$C_{ov} = \left(C_0 + \frac{I}{Q_s}\right) \tag{16}$$

Similar to the resuspension case, the terms accounting for the deposition effect are not included. Substituting Eq. (16) into Eq. (12) and rearranging yield

$$\frac{dC_i}{dt} + bC_i = a\left(C_0 + \frac{I}{Q_s}\right) \tag{17}$$

The solution to Eq. (17) is

$$C_i(t) = e^{-bt}C_i(0) + \frac{a\left(C_0 + I/Q_s\right)}{b}\left(1 - e^{-bt}\right) \tag{18}$$

4.2.2. Case study

Based on Eqs. (15) and (18), the influences of resuspension and injection in the ventilation duct toward indoor particle concentration are explored through two hypothetical cases for resuspension and injection, respectively. The considered BW agent is *B. anthracis* which is a Gram-positive, spore-forming bacillus with the approximate size of 1 μm × 5 μm [39].

Table 4
The parameters for calculating the resuspension rate.

Parameters	Meaning	Unit	Value	Source
d_p	Particle diameter	μm	3	[39]
A_{132}	Hamaker constant	J	7.12×10^{-20} [a]	[14]
u^*	Friction velocity	m/s	0.247	Section 3.1.3
ρ_p	Particle density	kg/m^3	1200	[8]
ρ_a	Air density	kg/m^3	1.2	[40]
R_q	Surface roughness	μm	5	[8]

[a] : $A_{132} = \sqrt{A_{11}A_{22}}$, where $A_{11} = 6.5 \times 10^{-20}$ J and $A_{22} = 7.8 \times 10^{-20}$ J are the Hamaker constant of particle and surface, respectively [14].

4.2.2.1. Resuspension case. In this case, 10 grams of *B. anthracis* spores are covertly dosed onto the duct floor when the ventilation is off. The ventilation duct is made of plastic with the cross-sectional dimension of 0.25 m (W) × 0.25 m (H) [17]. It is assumed that the relationship between the friction velocity and free stream velocity in the wind tunnel experiments of this work also holds. The resuspension rate is obtained as the average of the emp1 (Eq. (7)) from [15] and the model II-A (Eq. (8)) from [14]. The parameters needed for calculating the resuspension rate are listed in Table 4. The penetration coefficients through bends (p_b and p_{bi}) are approximated to be 100% for the considered airflow condition and agent size [36]. The duct lengths (x and x_{vi}) are assumed to be 20 m. The parameters used for modeling the airborne concentration are summarized in Table 5. The modeled indoor airborne concentration within a 5-h period is shown by Fig. 7(a).

4.2.2.2. Injection case. In this case, 10 grams of *B. anthracis* spores are directly dosed into the duct during a 1-min period when the ventilation is on. The relevant parameters are listed in Table 5. Similar to the resuspension case, the airborne concentration variation during a 5-h period is modeled as shown by Fig. 7(b).

For the resuspension case, it is shown that the airborne concentration indoors increases to the level of 4.9×10^5 #/m^3 at about 0.005 h and then declines quickly up to about 2 h followed by a slow decrease afterwards. The airborne concentration only decreases by one half (from 1300 #/m^3 to 530 #/m^3) for the 2–5 h period. These phenomena are related to the fact that the resuspension decays as time in the manner of power law relation: the decay rate of resuspension rate decreases as time. For the injection case, it is shown that the airborne concentration increases to the level of 1.37×10^7 #/m^3 during the injection period (1 min) and then declines exponentially afterwards due to the loss mechanisms (e.g., deposition and ventilation). After 2.2 h, the airborne concentration indoors goes down to about 1 #/m^3.

Comparing Fig. 7(a) and (b) shows that the variation patterns are different between the two cases. Under the same BW agent dosage, the resultant peak airborne concentration indoors for the resuspension case is about one thirtieth of that for the injection case. On the other hand, the airborne concentration indoors after 2 h for the resuspension case is more than one thousand times of that for the injection case. As a whole, the resuspension case intends to prolong occupants' exposure to harmful agents, while the injection case intends to produce a larger peak concentration.

Table 5
The parameters required by modeling of two cases.

Parameter	Meaning	Resuspension case	Injection case	Source
α_a (1/s)	Air exchange rate	1.39×10^{-3}	1.39×10^{-3}	[41]
R_r	Fraction of recirculated air	0.8	0.8	[17]
η_r	Filter efficiency	0.8	0.8	[35]
p_b and p_{bi}	Penetration through bend(s)	1	1	[36]
d_v and d_{vi}	Deposition loss in the duct	0.98	0.98	–
v_{df} (m/s)	Deposition velocity onto floor	2.0×10^{-3}	2.0×10^{-3}	[37]
v_{dw} (m/s)	Deposition velocity onto wall	6.0×10^{-5}	6.0×10^{-5}	[37]
v_{dc} (m/s)	Deposition velocity onto ceiling	3.0×10^{-6}	3.0×10^{-6}	[37]
x and x_{vi} (m)	Duct lengths	20	20	–
A_f (m^2)	Area of floor	64	64	–
A_w (m^2)	Area of wall	80	80	–
A_c (m^2)	Area of ceiling	64	64	–
V (m^3)	Indoor space volume	160	160	–
β_b (m^3/s)	Breathing rate	2.83×10^{-4}	2.83×10^{-4}	[42]
n_p	Number of occupants	3	3	–
$C_i(0)$ (#/m^3)	Initial indoor airborne concentration	0	0	–
C_o (#/m^3)	Pathogen concentration upstream the resuspension or injection site	0	0	–
Λ (1/s)	Resuspension rate	$1.3 \times 10^{-3} t^{-0.97}$	–	[14,15]
I (#/s)	Injection rate	0	982,438,750	–

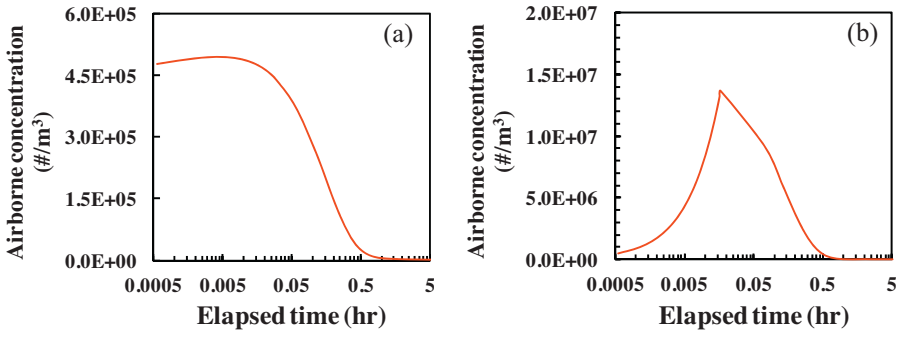

Fig. 7. The variation of airborne pathogen concentrations for (a) resuspension case and (b) injection case.

5. Conclusions

In this work, the models of particle concentration dynamics in the ventilation duct following a resuspension or injection event were developed from the mass balance model. The proposed models were validated against a series of wind tunnel experiments. The variation patterns of particle concentration in the duct are different between the resuspension and injection cases, suggesting the necessity of correctly indentifying the actual way of release. The proposed models could potentially serve as such a tool of indentifying the way of release and provide the foundation for predicting the BW agent concentration in the supply air and in the occupied space. The proposed ventilation duct models for resuspension and injection were applied to derive the indoor airborne particle concentration models using the indoor airborne mass balance model. The effects of resuspension and injection events in the duct on indoor airborne particle concentration were examined in terms of two hypothetical cases using the derived models. Under the same BW agent dosage, the resuspension case prolongs occupants' exposure to harmful agents whereas the injection case produces a higher peak concentration.

Acknowledgment

This work is financially supported jointly by A*STAR-MND Green Building Joint Grant through grant no. 1121760021 and NRF-CREATE SinBerBEST programme.

Appendix A. Model Derivation

Derivation of the solution of the equation

$$A\frac{\partial C(x,t)}{\partial t}+Q_s\frac{\partial C(x,t)}{\partial x}=-v_{dv}C(x,t)P \tag{A.1}$$

with the boundary condition of

$$C(x,t)|_{x=0}=C_0+\frac{N_0Sr_1t^{-r_2}}{Q_s} \tag{A.2}$$

and the initial condition of

$$C(x,t)|_{t=0}=C_{t0}. \tag{A.3}$$

Make a coordination transformation to t and x with $\xi=t$, $\eta=Q_st-Ax$ and have $\omega(\xi,\eta)=C\left(x\left(\xi,\eta\right),t(\xi,\eta)\right)$. Hence, we will have

$$\frac{\partial C}{\partial t}=\frac{\partial\omega}{\partial\xi}\frac{\partial\xi}{\partial t}+\frac{\partial\omega}{\partial\eta}\frac{\partial\eta}{\partial t}=\frac{\partial\omega}{\partial\xi}+Q_s\frac{\partial\omega}{\partial\eta} \tag{A.4}$$

and

$$\frac{\partial C}{\partial x}=\frac{\partial\omega}{\partial\xi}\frac{\partial\xi}{\partial x}+\frac{\partial\omega}{\partial\eta}\frac{\partial\eta}{\partial x}=-A\frac{\partial\omega}{\partial\eta}. \tag{A.5}$$

And Eq. (A.1) becomes

$$\frac{\partial\omega}{\partial\xi}+\frac{v_{dv}P}{A}\omega=0 \tag{A.6}$$

which can be further changed to

$$\frac{\partial}{\partial\xi}\left(e^{\frac{v_{dv}P}{A}\xi}\omega\right)=0. \tag{A.7}$$

Integrating Eq. (A.7) with respect to ξ results in

$$e^{\frac{v_{dv}P}{A}\xi}\omega=f(\eta) \tag{A.8}$$

which gives

$$\omega=f(\eta)e^{-\frac{v_{dv}P}{A}\xi}. \tag{A.9}$$

Substituting $\xi(x,t)$ and $\eta(x,t)$ back into Eq. (A.9) leads to

$$C(x,t)=f(Q_st-Ax)e^{-\frac{v_{dv}P}{A}x}. \tag{A.10}$$

Based on the boundary condition, Eq. (A.2), the differentiable function f in Eq. (A.10) can be defined and Eq. (A.10) becomes

$$C(x,t)=\frac{N_0Sr_1}{Q_s\left(t-Ax/Q_s\right)^{r_2}}e^{-\frac{v_{dv}Px}{Q_s}}+C_0e^{-\frac{v_{dv}Px}{Q_s}}. \tag{A.11}$$

Obviously, if $t\le Ax/Q_s$, Eq. (A.11) will become unreasonable. Actually, when $t\le Ax/Q_s$, the location x will not be affected by the particle resuspension and upstream concentration C_0. Considering the initial condition, Eq. (A.3), the solution of Eq. (A.1) should be finalized as

$$C(x,t)=\begin{cases}C_{t0} & \left(0<t\le\frac{Ax}{Q_s}\right)\\ \frac{N_0Sr_1}{Q_s\left(t-Ax/Q_s\right)^{r_2}}e^{-\frac{v_{dv}Px}{Q_s}}+C_0e^{-\frac{v_{dv}Px}{Q_s}} & \left(\frac{Ax}{Q_s}<t\right)\end{cases}. \tag{A.12}$$

Appendix B. Friction velocity determination

Before the measurement of boundary layer velocity profile, the pitot-tube with the manometer was used to calibrate the hotwire anemometer following the method of [43]. Then, the boundary layer velocity profile was measured by traversing the anemometer probe from the height of 0.1 to 0.27 mm at the increment of 0.01 mm for each of six free stream velocities: 1.85, 2.45, 3.07, 3.59, 4.19 and 5.20 m/s. For turbulent boundary layers, the velocity profile can be formulated with the Prandtl equation:

$$u=\frac{u^*}{\kappa}\ln\left(\frac{z}{z_0}\right), \tag{B.1}$$

where κ is the von Kármán constant ($\kappa=0.41$), z is the vertical distance from the surface and z_0 is the aerodynamic roughness length. In order to determine the friction velocity, the recorded velocity data would be fitted to the Prandtl equation. And similar to the method introduced by [44], the velocity profile is shown as $\ln(z)$ versus u (Fig. B.1(a)) and the friction velocity corresponding to each free stream velocity could be found based on the slope of fitted curve. Finally, a linear relationship between the friction velocity and free stream velocity could be found as illustrated in Fig. B.1(b), where $u^*=0.0710u-0.0056$ with the residual sum of square $R^2=0.988$.

Appendix C. Lengthwise spatial concentration variation

The concentration variation along the duct after resuspension and injection at different time points (10, 20, 30 s) is explored using the proposed models. The dosing location is located at the origin (0 m) of duct length. For the resuspension case, 2 μm particles on plastic substrate are used. For the injection case, 2 μm particles are used with the adjusted injection duration of 20 s. All other parameters required by modeling are kept the same as above. The results are shown in Fig. C.1.

It is shown by Fig. C.1(a) that the particle concentration increases along with the duct until the concentration peak which is the furthest location the airflow carrying resuspended particles could reach by the time. The concentration peak decreases with time (10–30 s) because more particles are lost due to deposition. This decrease in concentration is about 16% of the peak concentration, suggesting that deposition has a minor impact on the concentration for 2 μm particles, compared to primary resuspension. Further down from the concentration peak, the concentration is not affected by the primary resuspension but decreases slowly due to deposition, compared to the initial concentration, C_{t0}.

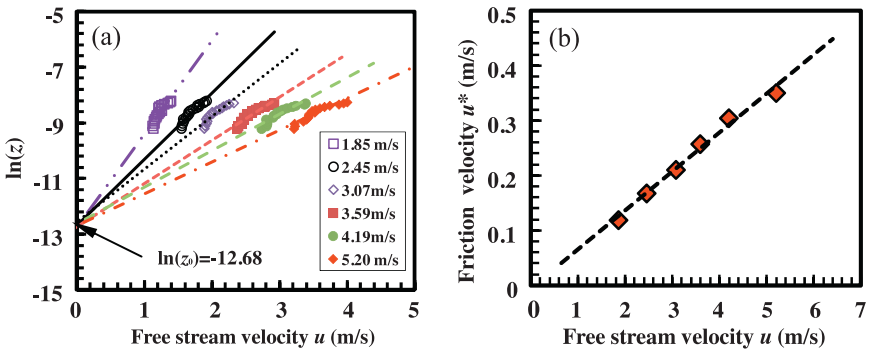

Fig. B.1. (a) The boundary layer velocity profiles at various free stream velocities. (b) The relationship between the friction velocity and free stream velocity.

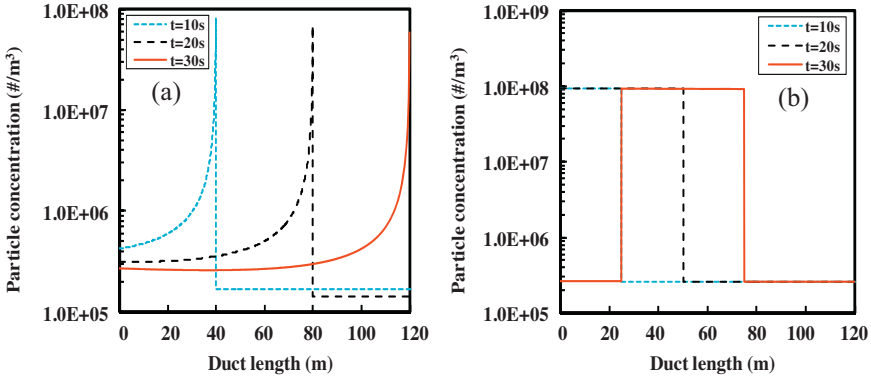

Fig. C.1. The spatial variation of particle concentration in the duct at various time points (10, 20 and 30 s) after (a) resuspension and (b) injection.

Fig. C.1(b) shows that the concentration variation exhibits a rectangular pulse response in the injection case. The airflow pushes the injected particles forward and a concentration pulse is formed spanning the duct length of airflow velocity × injection duration. The pulse moves downstream as the time goes on and the magnitude of the pulse decreases due to particle deposition. However, the concentration decrease due to deposition is minor compared to the pulse peak concentration, suggesting the weak effect of deposition in reducing concentration. Comparing Fig. C.1(a) and (b) shows that the concentration variation patterns in these two cases are different, indicating that the way of dosing in case of bioterrorist attack has a huge impact on the way that the BW agents are delivered downstream in the ventilation system. This might significantly influence the corresponding control and prevention measures (e.g., risk assessment) to be used. The above conclusions also hold for the case of larger particles (e.g., 10 μm, not shown here to avoiding repetition).

References

[1] A.F. Kaufmann, M.I. Meltzer, G.P. Schmid, The economic impact of a bioterrorist attack: are prevention and postattack intervention programs justifiable? Emerg. Infect. Dis. 3 (1997) 83.
[2] P.F. Deisler, A perspective: risk analysis as a tool for reducing the risks of terrorism, Risk Anal. 22 (2002) 405–413.
[3] G. Sze To, M. Wan, C.Y. Chao, F. Wei, S.C. Yu, J. Kwan, A methodology for estimating airborne virus exposures in indoor environments using the spatial distribution of expiratory aerosols and virus viability characteristics, Indoor Air 18 (2008) 425–438.
[4] G. Sze To, C. Chao, Review and comparison between the Wells–Riley and dose–response approaches to risk assessment of infectious respiratory diseases, Indoor Air 20 (2010) 2–16.
[5] B.P. Thompson, L.C. Bank, Survey of bioterrorism risk in buildings, J. Archit. Eng. 14 (2008) 7–17.
[6] T. Kean, The 9/11 Commission Report: Final Report of the National Commission on Terrorist Attacks Upon the United States, US Independent Agencies and Commissions, 2011.
[7] V.P. Reshetin, J.L. Regens, Simulation modeling of anthrax spore dispersion in a bioterrorism incident, Risk Anal. 23 (2003) 1135–1145.
[8] P. Krauter, A. Biermann, Reaerosolization of fluidized spores in ventilation systems, Appl. Environ. Microbiol. 73 (2007) 2165–2172.
[9] E.B. Sansone, M.W. Slein, Redispersion of indoor surface contamination: a review, J. Hazard. Mater. 2 (1977) 347–361.
[10] M. Zuraimi, Is ventilation duct cleaning useful? A review of the scientific evidence, Indoor Air 20 (2010) 445–457.
[11] B. Zhou, B. Zhao, Z. Tan, How particle resuspension from inner surfaces of ventilation ducts affects indoor air quality—a modeling analysis, Aerosol Sci. Technol. 45 (2011) 996–1009.
[12] C. McKenna Neuman, J.W. Boulton, S. Sanderson, Wind tunnel simulation of environmental controls on fugitive dust emissions from mine tailings, Atmos. Environ. 43 (2009) 520–529.
[13] J.A. Roney, B.R. White, Estimating fugitive dust emission rates using an environmental boundary layer wind tunnel, Atmos. Environ. 40 (2006) 7668–7685.
[14] Y. Kim, A. Gidwani, B.E. Wyslouzil, C.W. Sohn, Source term models for fine particle resuspension from indoor surfaces, Build. Environ. 45 (2010) 1854–1865.
[15] G.A. Loosmore, Evaluation and development of models for resuspension of aerosols at short times after deposition, Atmos. Environ. 37 (2003) 639–647.
[16] M. Reeks, J. Reed, D. Hall, On the resuspension of small particles by a turbulent flow, J. Phys. D: Appl. Phys. 21 (1988) 574.
[17] M.R. Sippola, W.W. Nazaroff, Modeling particle loss in ventilation ducts, Atmos. Environ. 37 (2003) 5597–5609.
[18] J. Chang, K.K. Foarde, D.W. VanOsdell, Assessment of fungal (*Penicillium chrysogenum*) growth on three HVAC duct materials, Environ. Int. 22 (1996) 425–431.
[19] H. Jiang, L. Lu, K. Sun, Simulation of particle deposition in ventilation duct with a particle–wall impact model, Build. Environ. 45 (2010) 1184–1191.
[20] S. Wang, B. Zhao, B. Zhou, Z. Tan, An experimental study on short-time particle resuspension from inner surfaces of straight ventilation ducts, Build. Environ. 53 (2012) 119–127.
[21] K. Sun, L. Lu, H. Jiang, A numerical study of bend-induced particle deposition in and behind duct bends, Build. Environ. 52 (2012) 77–87.
[22] G. Klimchitskaya, U. Mohideen, V. Mostepanenko, Casimir and van derWaals forces between two plates or a sphere (lens) above a plate made of real metals, Phys. Rev. A 61 (2000) 062107.
[23] K. Al-Malah, J. McGuire, V. Krisdhasima, P. Suttiprasit, R. Sproull, Ellipsometric evaluation of β-lactoglobulin adsorption onto low- and high-energy materials, Biotechnol. Progr. 8 (1992) 58–66.
[24] J.N. Israelachvili, Intermolecular and Surface Forces, third ed. (revised), Academic Press, 2011.
[25] S. You, M.P. Wan, Modeling and Experimental Investigation of Human-walking-induced Aerosol Resuspension, Indoor Built Environ.,.(Unpublished results).

[26] W. Kowalski, W. Bahnfleth, A. Musser, Modeling immune building systems for bioterrorism defense, J. Archit. Eng. 9 (2003) 86–96.
[27] M.R. Sippola, W.W. Nazaroff, Experiments measuring particle deposition from fully developed turbulent flow in ventilation ducts, Aerosol Sci. Technol. 38 (2004) 914–925.
[28] S.-R. Lee, T.M. Holsen, S. Dhaniyala, Design and development of novel large particle inlet for PM larger than 10 μm (PM > 10), Aerosol Sci. Technol. 42 (2008) 140–151.
[29] J.H. Lee, K. Ahn, S.M. Kim, K.S. Jeon, J.S. Lee, I.J. Yu, Continuous 3-day exposure assessment of workplace manufacturing silver nanoparticles, J. Nanopart. Res. 14 (2012) 1–10.
[30] T. Hussein, K. Hämeri, M.S. Heikkinen, M. Kulmala, Indoor and outdoor particle size characterization at a family house in Espoo—Finland, Atmos. Environ. 39 (2005) 3697–3709.
[31] A.R. Ferro, R.J. Kopperud, L.M. Hildemann, Source strengths for indoor human activities that resuspend particulate matter, Environ. Sci. Technol. 38 (2004) 1759–1764.
[32] T. Hussein, H. Korhonen, E. Herrmann, K. Hämeri, K.E. Lehtinen, M. Kulmala, Emission rates due to indoor activities: indoor aerosol model development, evaluation, and applications, Aerosol Sci. Technol. 39 (2005) 1111–1127.
[33] W.W. Nazaroff, G.R. Cass, Mathematical modeling of indoor aerosol dynamics, Environ. Sci. Technol. 23 (1989) 157–166.
[34] T. Schneider, J. Kildes, A two compartment model for determining the contribution of sources, surface deposition and resuspension to air and surface dust concentration levels in occupied rooms, Build. Environ. 34 (1999) 583–595.
[35] W.J. Riley, T.E. McKone, A.C. Lai, W.W. Nazaroff, Indoor particulate matter of outdoor origin: importance of size-dependent removal mechanisms, Environ. Sci. Technol. 36 (2002) 200–207.
[36] A. McFarland, H. Gong, A. Muyshondt, W. Wente, N. Anand, Aerosol deposition in bends with turbulent flow, Environ. Sci. Technol. 31 (1997) 3371–3377.
[37] A.C.K. Lai, W.W. Nazaroff, Modeling indoor particle deposition from turbulent flow onto smooth surfaces, J. Aerosol Sci. 31 (2000) 463–476.
[38] A.C. Lai, Particle deposition indoors: a review, Indoor Air 12 (2002) 211–214.
[39] T.V. Inglesby, D.A. Henderson, J.G. Bartlett, M.S. Ascher, E. Eitzen, A.M. Friedlander, J. Hauer, J. McDade, M.T. Osterholm, T. O'Toole, Anthrax as a biological weapon, JAMA 281 (1999) 1735–1745.
[40] W.C. Hinds, Aerosol Technology: Properties, Behavior, and Measurement of Airborne Particles, second ed., Wiley-Blackwell, 1999.
[41] P.C. Wu, Y.Y. Li, C.M. Chiang, C.Y. Huang, C.C. Lee, F.C. Li, H.J. Su, Changing microbial concentrations are associated with ventilation performance in Taiwan's air-conditioned office buildings, Indoor Air 15 (2005) 19–26.
[42] W.J. Kowalski, Immune Building Systems Technology, McGraw Hill Professional, 2003.
[43] L. Chua, R. Antonia, The turbulent interaction region of a circular jet, Int. Commun. Heat Mass Transfer 13 (1986) 545–558.
[44] J.A. Roney, B.R. White, Definition and measurement of dust aeolian thresholds, J. Geophys. Res. 109 (2004) F01013.